Appl Phys A (2013) 110:853–856
DOI 10.1007/s00339-012-7164-3

Applied Physics A
Materials Science & Processing

Effect of prepulse laser wavelength on EUV emission from CO_2 reheated laser-produced Sn plasma

J.R. Freeman · S.S. Harilal · A. Hassanein · B. Rice

Received: 20 May 2011 / Accepted: 3 August 2012 / Published online: 25 August 2012
© Springer-Verlag 2012

Abstract We investigated the role of prepulse laser wavelength on extreme-ultraviolet (EUV) emission and ionic debris generation. A 6 ns Nd:YAG laser operating at 266 nm was used to generate a pre-plasma that was then reheated by a 35 ns CO_2 laser pumping pulse at 10.6 µm. At an ideal delay time, improvement in EUV conversion efficiency (CE) of up to 30 % was seen compared to the CE from the pumping pulse alone. It was also shown that the most probable Sn ion kinetic energies were reduced significantly with the use of a prepulse, however, ion fluence increased. These results were compared to those obtained using a 1064 nm prepulse.

1 Introduction

Extreme-ultraviolet (EUV) light from Sn plasma centered at 13.5 nm is the leading light source for the next generation of lithography due to the availability of Mo/Si multilayer mirrors offering 70 % reflectivity at this wavelength within 2 % bandwidth [1]. Other materials such as Li and Xe have been explored as potential light sources [2], but due to broad Sn emission centered at 13.5 nm caused by Sn^{8+}–Sn^{14+} ion transitions, Sn has become the main material of interest. Methods explored for exciting these ion transitions include discharge-produced plasma (DPP) and laser-produced plasma (LPP). Much research has been done to improve the efficiency and understand the plasma dynamics of these sources. However, due to the potential scalability for high volume manufacturing, LPP sources may have some advantages over DPP sources [3, 4]. In order to develop a viable EUV lithography system, highly efficient and low-debris LPP are needed. Techniques to improve conversion efficiency (CE) and mitigate optics-damaging debris from the Sn plasma are currently being pursued.

Nd:YAG lasers have been shown to provide high CE [5], but in 2005 Tanaka et al. [6] demonstrated the advantages of using a CO_2 laser for generating even higher CE. These advantages are attributed to the lower critical density of the CO_2 LPP, resulting in different plasma heating mechanisms which lead to improved EUV emission [7]. Laser parameters such as wavelength [7], intensity [8], and spot size [9] have all been shown to have significant effects on EUV emission and debris generation. Mass-limited targets [10, 11] have been shown to decrease plasma density, thereby decreasing self-absorption of EUV light and increasing CE, while also decreasing debris generation. Minimizing debris is necessary to extend the lifetime of collection optics that are damaged by energetic particles emanating from the plasma.

EUV emission from LPP can be increased using a double-pulse laser irradiation technique [10, 12]. In this scenario, a low-energy pulse creates a low-density pre-plasma from the target, which is then reheated by a high-energy pump pulse, generating an increase in EUV emission. In this work we compare the EUV emission from LPP using a double-pulse technique and comparing two different prepulse wavelengths. Maximum CE values are found by varying the delay between prepulse and the pumping pulse.

J.R. Freeman (✉) · S.S. Harilal · A. Hassanein
Center for Materials Under eXtreme Environment, School of Nuclear Engineering, Purdue University, West Lafayette, IN 47906, USA
e-mail: freemaj@purdue.edu

S.S. Harilal
e-mail: hari@purdue.edu

A. Hassanein
e-mail: hassanein@purdue.edu

B. Rice
SEMATECH Inc., Albany, NY 12203, USA
e-mail: bryan.rice@sematech.org

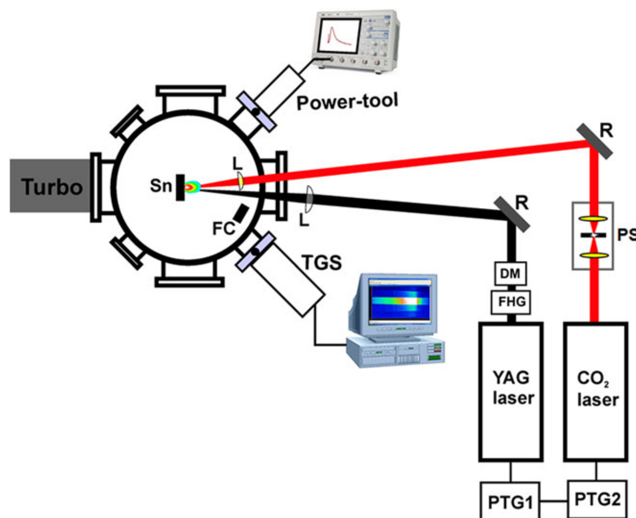

Fig. 1 Schematic illustration of the experimental setup (PTG, programmable timing generator; FHG, fourth-harmonic generator; DM, dichroic mirror; PS, plasma shutter; R, reflective optics; L, lens; FC, Faraday cup; TGS, transmission grating spectrograph). Nd:YAG laser generates a pre-plasma that is reheated by the CO_2 laser at a set time delay. Triggering of both lasers is performed using timing generators

The EUV spectra emitted from the plasma are studied and compared to determine the source of increased emission. Sn ion kinetic energy distributions are also compared to determine the effect of the pre-plasma on ion dynamics.

2 Experimental setup

The setup of our experimental facility can be seen in Fig. 1. A planar Sn target is irradiated by a 6 ns full width half maximum (FWHM) prepulse Nd:YAG laser operating at its fourth (266 nm) harmonic to generate a pre-plasma. The pre-plasma is subsequently reheated by a 35 ns FWHM pumping pulse transversely excited atmospheric (TEA) CO_2 laser operating at 10.6 μm. A plasma shutter was used to eliminate the long nitrogen tail of the CO_2 laser pulse [13]. The delay between prepulse and pumping pulse is controlled by a combination of two timing generators used to run the flash lamps of the Nd:YAG laser to minimize thermal lensing effects and to trigger both lasers. Both lasers are aligned at angles of 5° with respect to the target normal inside a vacuum chamber evacuated to a pressure of $\sim 10^{-6}$ Torr. Spot sizes used were 100 μm and 225 μm for Nd:YAG and CO_2 lasers, respectively. The target was incremented to a fresh spot for each laser shot.

Ion dynamics were recorded using a Faraday cup (FC) biased with −31 V DC voltage and positioned 19.8 cm from the target at an angle of 25° with respect to target normal. EUV CE was calculated over 2π sr solid angle using an absolutely calibrated EUV Power Tool employing two 150 nm Zr filters, one Mo/Si multilayer mirror, and EUV photodiode, in order to collect 13.5 nm light within 2 % bandwidth. Signals from the FC and EUV Power Tool were recorded using a 1 GHz digital oscilloscope. EUV emission spectra were obtained with EUV transmission grating spectrograph (TGS) with 10,000 lines/mm silicon nitride grating, connected to a back-illuminated EUV-sensitive charge-coupled device (CCD).

3 Results and discussion

Our previous work [12] has justified the use of the Nd:YAG laser as the prepulse and the CO_2 laser as the pumping pulse for double-pulse experiments aiming to increase EUV emission. This conclusion was made through consideration of critical densities of Nd:YAG and CO_2 LPP [14] with the goal of efficient pumping pulse and pre-plasma coupling. We observed an increase in CE of 40 % using a 1064 nm Nd:YAG prepulse and CO_2 pumping pulse. It was hypothesized that by increasing the density of the pre-plasma, pumping pulse and pre-plasma coupling could be improved, resulting in enhanced EUV emission. To increase pre-plasma density, the shorter wavelength (266 nm) fourth-harmonic of the Nd:YAG laser was chosen. Due to a plasma critical density greater than one order of magnitude larger than that for the 1064 nm Nd:YAG, the 266 nm Nd:YAG laser would provide a denser pre-plasma for improved coupling with the pumping pulse. In this study we compared the differences between 266 nm and 1064 nm Nd:YAG prepulses with the 10.6 μm CO_2 laser being the pumping pulse. The pumping pulse energy was 90 mJ with power density of 6.5×10^9 W/cm^2 throughout the experiments and the prepulse was 15 mJ energy with 3.2×10^{10} W/cm^2 power density. Spectra and time-of-flight (TOF) data were taken for the individual prepulse and pumping pulse for comparisons to the double-pulse data.

A delay range scan was performed to identify the optimum delay between prepulse and pumping pulse at which the maximum CE was realized. Spatial alignment of the pumping pulse with respect to the pre-plasma is critical, as minute changes can affect CE and delay times due to expansion in different directions and coupling with the pumping pulse. The main idea in the adjustment of the prepulse plasma and time of the delay is based on coupling the formed and expanded pre-plasma to the spot size of the pumping laser [15]. The effect of the delay time is shown in Fig. 2 for the 266 nm prepulse. Trends in the 1064 nm prepulse delay curve were very similar. At the peak delay, CE was found to be 3.0 % for the 266 nm prepulse, similar to that found with a 1064 nm prepulse with identical laser parameters. This corresponds to an increase in CE of 30 % compared to CE of the pumping pulse alone, which

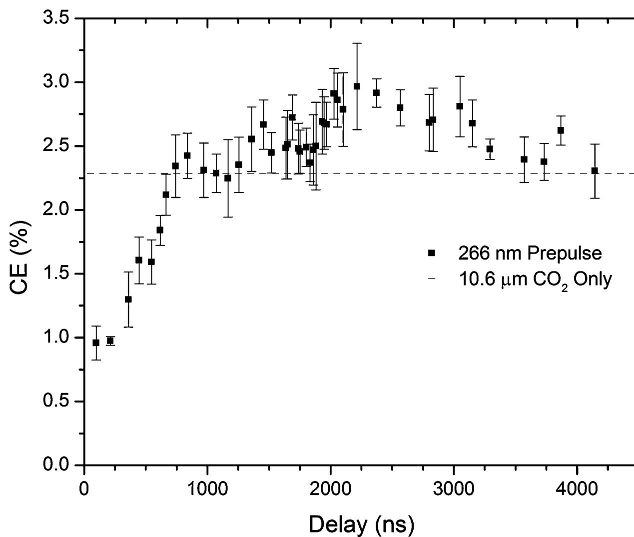

Fig. 2 Dependence of CE on delay time for 266 nm prepulsed shots. CE from the pumping pulse alone is 2.3 %

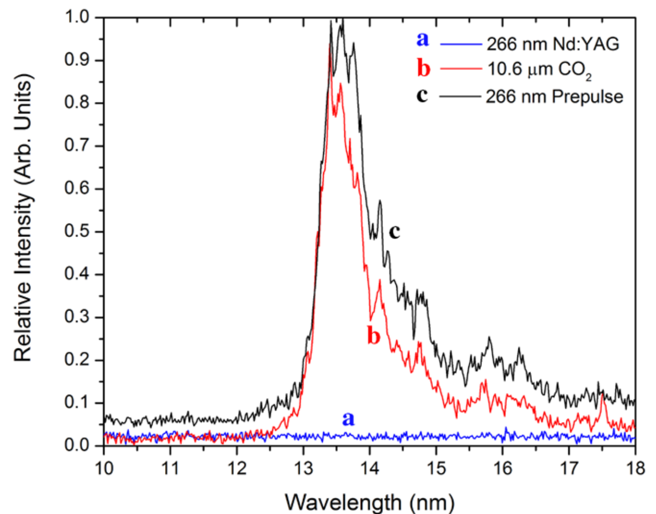

Fig. 3 EUV spectral data using transmission grating spectrograph and EUV-sensitive camera for 266 nm prepulse at its peak delay compared to the individual pumping pulse and prepulse alone. Pumping pulse interaction with the pre-plasma resulted in increased spectral intensity and broadening of the UTA

was 2.3 %, signifying that both prepulse wavelengths can produce comparable CE. The 30 % increase in CE is comparable to that found in our previous work investigating the 1064 nm prepulse [12].

By examining the trends of the data, it is shown that at short delays between prepulse and pumping pulse, CE is very low. As the delay increases, CE begins to increase. The decrease at short delays can be attributed to poor coupling of the pre-plasma and pumping pulse for generating EUV emission. Once the delay increases, the pre-plasma is less dense and conditions for EUV generation improve. The drop in CE for the 266 nm prepulse was more drastic than that of the 1064 nm prepulse because the 266 nm pre-plasma is denser and more self-absorption within the pre-plasma plume can be expected. At the peak delay, the pre-plasma plume is dense enough to absorb radiation from the pumping pulse, but not dense enough to absorb EUV photons generated during reheating. Corresponding to this peak delay, the pre-plasma plume can be expected to contain mostly neutral Sn atoms and small clusters in the cold plasma to provide a low-density target for the pumping pulse that can generate, as well as transmit, EUV light. After the optimum peaks, CE values from both prepulse wavelengths gradually decrease as the pre-plasma plume disperses and the pumping pulse interacts mainly with the target surface.

EUV emission spectra can be seen in Fig. 3. Prepulse spectra were obtained using the optimum delay between prepulse and pumping pulse. From the spectra, CE can be understood as the area enclosed by the spectra within 2 % bandwidth centered at 13.5 nm. The spectra show that for the 266 nm prepulse, increases in spectral intensity as well as broadening of the unresolved transition array (UTA) on the high-wavelength, low-energy side are responsible for the increases in CE seen in Fig. 2. This indicates that lower-energy ionic states are more efficiently excited. The 1064 nm prepulse showed similar enhancements with negligible difference to that of the 266 nm prepulse and was in agreement with our previous results [12]. Emission from the individual prepulses was shown to be negligible, so improvements in the prepulse spectra can be attributed solely to interaction of the pumping pulse with the pre-plasma and not from contributions by the pre-plasma's own emission. However, it should be pointed out that out-of-band (OoB) emission worsens spectral purity and should be avoided, as it results in increased heat load to collection optics. Figure 3 shows that a prepulse provides increased spectral intensity and broadening of the UTA, resulting in improved CE, but a difference between prepulse wavelengths could not be discerned from their spectra [12].

Figure 4 shows the ion kinetic energy distributions from Sn plasmas to compare prepulse wavelengths. Most probable ion energies are shown to be approximately 55 eV and 45 eV for 266 nm and 1064 nm prepulsed plasmas, respectively. Ions with energies in this region were produced by the pumping pulse interacting with the target surface. Expansion of ions in this plasma is slowed greatly due to confinement by the existing pre-plasma. This results in enhanced recombination and substantial lowering of ion energies. Both prepulse energy distributions display a higher-energy plateau region. This region can be attributed to ions from the pre-plasma, as well as those in the pre-plasma that are reheated by the pumping pulse. As a comparison, ion energy distributions from the pumping pulse alone are centered near 2.25 keV. This signifies a reduction in most probable ion energy of nearly two orders of magnitude. This may decrease sputtering and interlayer mixing of multilayer col-

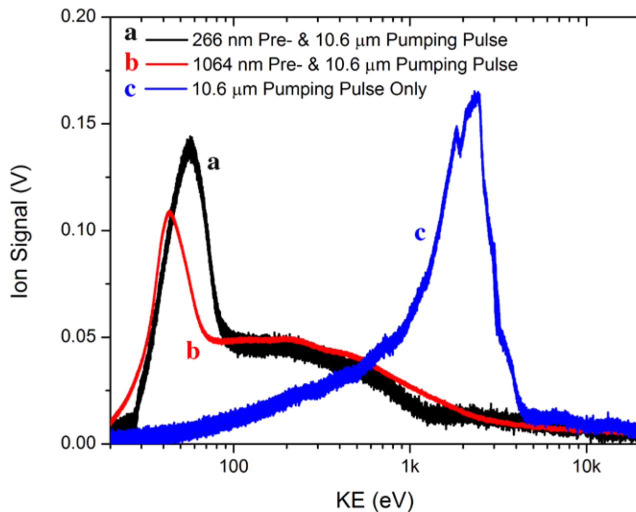

Fig. 4 Ion kinetic energy spectra comparing different prepulse wavelengths at their respective peak delays with the spectra produced by the pumping pulse alone. By using a prepulse before the pumping pulse, ions generated by the pumping pulse are slowed down significantly

lection optics exposed to this debris. The total ion fluence from both prepulsed plasmas is shown to be comparable. However, total ion fluence from the prepulsed plasmas is about 2.65 times greater than that from the pumping pulse alone, albeit consisting of mostly lower-energy ions. Despite their higher ion fluencies prepulsed plasmas, regardless of prepulse wavelength used, provide less energetic ions and it should be noted that it is much easier to mitigate these lower velocity ions using electric or magnetic field mitigating schemes.

4 Conclusion

Detailed analysis using a combination of 266 nm Nd:YAG prepulse and CO_2 laser pumping pulse for a LPP EUV source at 13.5 nm was conducted and compared with results using a 1064 nm prepulse. It was found that both prepulse wavelengths produced similar EUV emission enhancements of 30 % compared to emission from the pumping pulse alone. The EUV emission spectra using both prepulse wavelengths showed similar increases in spectral intensity and broadening of the UTA and are the cause of the increased emission. Ion kinetic energy distributions showed substantial reduction of ion energy by employing the prepulse. This observation was true for both prepulse wavelengths (266 nm and 1064 nm) investigated. The reduction in ion energy is important for future commercial systems, as sputtering and interlayer mixing of multilayer collection optics would be greatly mitigated and operating lifetimes of optics may be extended, however, the increase in ion fluence could offset these benefits. In conclusion, there is shown to be negligible difference between the two prepulse wavelengths studied. For practical purposes, a 1064 nm prepulse may be desired for its availability and ease of use.

Acknowledgements This work is partially supported by SEMATECH Inc. and Purdue University.

References

1. J.S. Taylor, R. Soufli, Specification, fabrication, testing, and mounting of EUVL optical substrates, in *EUV Lithography*, ed. by V. Bakshi (SPIE/Wiley, Bellingham/Hoboken, 2009), p. 188
2. V. Bakshi, EUV source technology: challenges and status, in *EUV Sources for Lithography*, ed. by V. Bakshi (SPIE—The International Society for Optical Engineering, Bellingham, 2006), p. 7
3. V.Y. Banine, K.N. Koshelev, G.H.P.M. Swinkels, J. Phys. D Appl. Phys. **44**, 253001 (2011)
4. V. Sizyuk, A. Hassanein, V. Bakshi, J. Micro/Nanolithogr. MEMS MOEMS **6**, 043003 (2007)
5. R.C. Spitzer, R.L. Kauffman, T. Orzechowski, D.W. Phillion, C. Cerjan, J. Vac. Sci. Technol. B **11**, 2986 (1993)
6. H. Tanaka, A. Matsumoto, K. Akinaga, A. Takahashi, T. Okada, Appl. Phys. Lett. **87**, 041503 (2005)
7. J. White, P. Dunne, P. Hayden, F. O'Reilly, G. O'Sullivan, Appl. Phys. Lett. **90**, 181502 (2007)
8. R.W. Coons, S.S. Harilal, D. Campos, A. Hassanein, J. Appl. Phys. **108**, 063306 (2010)
9. S.S. Harilal, R.W. Coons, P. Hough, A. Hassanein, Appl. Phys. Lett. **95**, 221501 (2009)
10. S. Fujioka, M. Shimomura, Y. Shimada, S. Maeda, H. Sakaguchi, Y. Nakai, T. Aota, H. Nishimura, N. Ozaki, A. Sunahara, K. Nishihara, N. Miyanaga, Y. Izawa, K. Mima, Appl. Phys. Lett. **92**, 241502 (2008)
11. S.S. Harilal, M.S. Tillack, Y. Tao, B. O'Shay, R. Paguio, A. Nikroo, Opt. Lett. **31**, 1549 (2006)
12. J.R. Freeman, S.S. Harilal, A. Hassanein, J. Appl. Phys. **110**, 083303 (2011)
13. N. Hurst, S.S. Harilal, Rev. Sci. Instrum. **80**, 035101 (2009)
14. S.S. Harilal, T. Sizyuk, A. Hassanein, D. Campos, P. Hough, V. Sizyuk, J. Appl. Phys. **109**, 063306 (2011)
15. A. Hassanein, T. Sizyuk, V. Sizyuk, S.S. Harilal, J. Micro/Nanolithogr. MEMS MOEMS **10**(3), 033002 (2011)